Chinese Journal of
POLYMER SCIENCE

ARTICLE

https://doi.org/
Chinese J. Polym. Sci. **2022**, *00*, 00–00

Effect of carboxymethyl cellulose (CMC) functionalization on dispersion, mechanical, and corrosion properties of CNT/epoxy nanocomposites

Dawei Zhang[a], Leonard Chia[a], and Ying Huang[a*]

[a] *Department of Civil, Construction and Environmental Engineering, North Dakota State University, Fargo 58108, USA*

◆ Electronic Supplementary Information

Abstract Carbon nanotube (CNT)/epoxy nanocomposites have a great potential of possessing many advanced properties. However, the homogenization of CNT dispersion is still a great challenge in the research field of nanocomposites. This paper applied a novel dispersion agent, carboxymethyl cellulose (CMC), to functionalize CNTs and improve CNT dispersion in epoxy. The effectiveness of the CMC functionalization was compared with mechanical mixing and another commonly used surfactant, sodium dodecylbenzene sulfonate (NaDDBS), regarding dispersion, mechanical and corrosion properties of CNT/epoxy nanocomposites with three different CNT concentrations (0.1%, 0.3%, and 0.5%). The experimental results of Raman spectroscopy, particle size analysis and transmission electron microscopy showed that CMC functionalized CNTs reduced CNT cluster sizes more efficiently than NaDDBS functionalized and mechanically mixed CNTs, indicating a better CNT dispersion. Compared to mechnaical mixed and NaDDBS functionalized CNTs, the peak particle size of CMC functionalized CNTs reduced as much as 54% (0.1 CNT concentration) and 16% (0.3 CNT concentration). Because of the better dispersion, it was found by compressive tests that CNT/epoxy nanocomposites with CMC functionalization resulted in 189% and 66% higher compressive strength, 224% and 50% higher modulus of elasticity than those with mechanical mixing and NaDDBS functionalization respectively (0.1 CNT cencentration). In addition, electrochemical corrosion tests also showed that CNT/epoxy nanocomposites with CMC functionalization achieved lowest corrosion rate (0.214 mpy), the highest corrosion resistance (201.031 Ω cm^2), and the lowest porosity density (0.011%).

Keywords CNT/epoxy composites; Carboxymethyl cellulose; Dispersion; Mechanical properties; Corrosion properties

Citation:.

INTRODUCTION

Epoxy resin has found its vital application in many industries as structural adhesives, anti-corrosive coatings, and composite matrix, due to its high specific strength, strong chemical stability, low shrinkage, and low cost.[1-3] However, those superb properties of epoxy resin are usually not fully utilized owing to the existence of micro-voids and pores produced during the curing process, which inevitably weaken the mechanical and anti-corrosive performance of epoxy resin as a whole.[4,5] Thus, a variety of reinforcing additives and fillers have been incorporated into epoxy resin to deviate, bridge, and pin the imperfections inside epoxy matrices.[6–8] Compared to traditional additives such as plastics and rubber which require a bulky amount of addition (normally 15 ~ 20 wt.%),[9,10] carbon nanotubes (CNTs), as the most popular representative of nanofillers have become more favorable as a reinforcing agent since only a modest amount of CNTs (less than 1%) is sufficient to provide a sound reinforcement to epoxy resin and other polymers.[11–13] Because of the intrinsic nature of CNTs (like extraordinarily high aspect ratio, strength, and young's modulus, as well as excellent thermal and chemical stability),[14,15] it is generally believed that CNT/epoxy nanocomposites are promising to achieve outstanding mechanical, thermal, and electrical properties.[16,17]

Although the immense potentials of CNT/epoxy nanocomposites have drawn tremendous research attention and industrial uses, there are still some challenges with CNT/epoxy nanocomposites, especially the unsatisfactory dispersion of CNTs.[18,19] CNTs are more likely to entangle and agglomerate with each other as CNT clusters in the epoxy resin, due to the high viscosity of epoxy resin as well as high aspect ratio and strong Van der Waals forces of CNTs.[20] It has been widely reported that the advanced properties of CNT/epoxy nanocomposites could be severely restricted owing to the agglomeration of CNTs.[21,22]

Various approaches have been developed attempting to overcome the obstacle of CNT dispersion and improve the functional performance of CNT/epoxy nanocomposites. Most of the approaches fall into two categories: mechanical mixing and CNT functionalization.[23,24] The mechanical mixing is the. most prevalent mixing method involving ultrasonic

---

* Corresponding authors: ying.huang@ndsu.edu (Y.H.)

stirring using a probe, ultrasonic bath,[25] high shear mixing,[26] and three-roll milling.[27] These mechanical mixing methods employ vibration and shear force to break up CNT clusters, however, they find difficulty of maintaining the uniform dispersion constantly.[28] In addition, some computational and experimental studies showed that mechanical mixing may cut off the CNT length during the separation of CNT clusters,[29,30] and short CNTs yield rather weak interfacial interactions with the surrounding epoxy matrix, which may seriously impair the reinforcing efficiency of CNTs.[31,32]

CNT functionalization involves CNT surface modification using chemical treatments such as concentrated acids,[33] amine,[34] and silane,[35] or physical treatments by various surfactants such as sodium dodecyl sulfate (SDS), sodium dodecylbenzene sulfonate (NaDDBS),[36] and Triton X-100.[37] Chemical or covalent functionalization creates chemical reactions on the surface of CNTs which promotes the compatibility between CNTs and polymers,[38] while physical or non-covalent functionalization is capable of greatly lowering the surface tension and effective overcome Van der Waals attractions among CNTs.[39,40] Although both treatments are effective in improving the CNT dispersion, literature found that chemical functionalization may produce structural damages on CNTs or deteriorate the fundamental properties of CNTs.[41] Therefore, since most surfactants rarely disturb the structure or inherency of CNTs, physical functionalization is particularly regarded as the preferred approach.[42,43]

Carboxymethyl cellulose (CMC) is an etherified derivative of cellulose and is soluble in water. Its aqueous solution has miscellaneous functions of thickening, binding, moisture retention, and colloidal protection in oil, food, pharmacy, and paper industries.[44] Previous work found that CMC is expected to improve the dispersion of single-walled CNTs and strengthen its interfacial interaction with polymeric materials as a physical functionalization agent.[45,46] But the current research only investigated the effect of CMC functionalization on the dispersion of CNTs into polymer matrix, there is no investigations on the mechanical and corrosion properties of CNT/epoxy nanocomposite with CMC functionalization. On the other hand, when proposing a new dispersion method or dispersion agent, most of the existing studies merely show the differences with and without the certain dispersion technique, there is limited research making comparisons among different dispersion approach categories and different dispersion agents.

This paper aimed at investigating the effect of a novel dispersion agent called CMC on the dispersion, mechanical, and corrosion properties of CNT/epoxy nanocomposites. The effects of mechanical mixing and another commonly used surfactant, NaDDBS were also exanimated for comparisons with the CMC functionalization. Three different CNT concentrations (0.1%, 0.3%, and 0.5%) were also considered throughout the study. Raman spectroscopy and particle size analysis were conducted to reflect the dispersion modifying effectiveness of CMC functionalization, while transmission electron microscopy (TEM) analyses were performed to actual reveal the dispersion state of CNTs with different dispersion methods. Mechanical properties were evaluated by compressive tests, while electrochemical tests by Tafel polarization were carried out to estimate the corrosion rate of CNT/epoxy nanocomposites.

EXPERIMENTAL

Materials

Multi-walled CNTs (purchased from Skyspring Nanomaterials Inc) with outside diameter of 50-100 nm, inside diameter of 5-10 nm, length of 5-20 µm, and purity >95% were manufactured by catalytic chemical vapor deposition and used as received. The epoxy resin used in this paper was supplied by East Coast Resin including a bisphenol A based resin and a polyamide curing agent. Both dispersion agents were acquired from Sigma-Aldrich Corp. The novel dispersion agent was sodium CMC (Prod. No. 419273, C28H30Na8O27), and NaDDBS (Prod. No. 289957, C18H29NaO3S) was selected as the commonly used surfactant for comparisons. In addition, the steel substrate used in the electrochemical corrosion test was A36 steel manufactured for general structural purposes (purchased from Mid America Steel Inc).

Dispersion Approaches

Three different dispersion approaches including mechanical mixing, CNT functionalization using NaDDBS and CMC were selected and compared in this paper. For CMC functionalization, 0.25g of CMC were initially dissolved into 50 ml deionized (DI) water, resulting in a 0.5% weight percentage of CMC aqueous solution.[46] The solution was simultaneously stirred on a magnetic stirrer at a speed of 1600 rpm to ensure a good dissolution of CMC. Then CNTs were gradually added into the solution with the same stirring process, followed by 24-hour mixing using a rotator in a test tube to ensure that CNTs and CMC had fully interacted with each other. Similar preparation procedures were also used to functionalize CNTs with NaDDBS, and the weight percentage of NaDDBS was also approximately 0.5%.[47] The detailed functionalization procedures are clearly demonstrated in Fig. 1. For mechanical mixing, CNT aqueous suspensions were mixed in a tube by ultrasonic bath, since ultrasonication is still the most accepted dispersion method. The ultrasonic duration was set as 90 minutes according to the literature,[28,29] and the tube was placed in water/ice bath to avoid temperature increases during ultrasonication. CNT/epoxy nanocomposites were fabricated following the same dispersion approaches as demonstrated above except the solution was replaced by curing agent. Subsequently, the mixture was thoroughly mixed with the resin by the magnetic stirrer. The volume ratio between the curing agent and resin was 1:1. After mixing, all the nanocomposites were placed in a curing condition of 32°C for the first 24 hours and then room temperature for at least 7 days before any testing.

Characterizations

The effects of different dispersion approaches on CNT dispersion were investigated by Raman spectroscopy and particle size analysis. Raman spectra of CNTs with three different dispersion approaches were recorded between 800 cm^{-1} to 2400 cm^{-1} using Aramis Confocal Raman Imaging System and Horiba Jobin Yvon's Raman spectrometer with a wavelength of 532 nm. Particle size analysis was employed using Particle Sizing Systems SPOS 780 by measuring the size distribution of diluted liquid suspensions. In addition, TEM were employed at Electron Microscopy Core of North Dakota State University to characterize the CNT dispersion states.

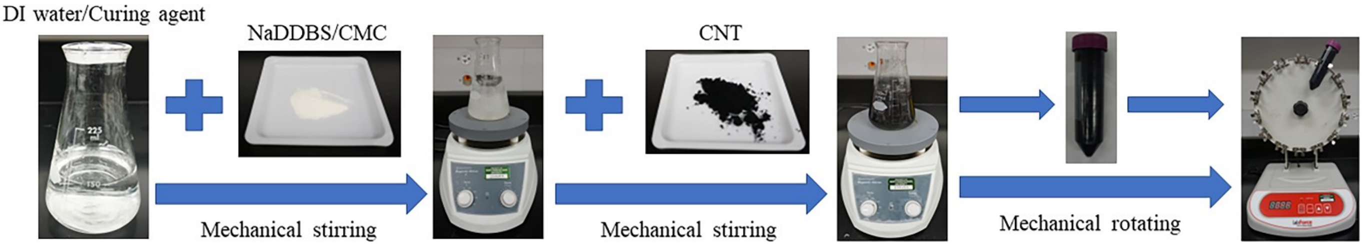

Fig. 1 CNT functionalization procedures using NaDDBS and CMC.

The mechanical properties of CNT/epoxy nanocomposites were evaluated by compressive test in accordance with ASTM D695-15 for compressive properties of rigid plastics. The dimension of the nanocomposite test specimen was 12.7 mm × 12.7 mm × 25.4 mm in the form of a right prism whose length is twice its principal width. After removing the specimen from the curing mold, all the surfaces of the specimen were machined carefully into smooth, flat parallel surfaces with sharp and clean edges. The loading machine of the compressive test was MTS Flex Test® SE loading frame, and test specimens were placed between the compressive tools so that the long axis of the specimen was in the alignment with the center line of the actuators. The experimental configuration is displayed in Fig. 2. The loading protocol was monotonic compressive loading at a displacement control mode of 1.3 mm/min. In addition, in order to examinate the effect of the three dispersion approaches on CNTs with different concentrations, 0.1%, 0.3%, and 0.5% CNT concentrations were prepared for each dispersion approach. Neat epoxy resin without CNT addition was also exanimated as the control group. For each combination of dispersion approaches and CNT concentrations, five identical specimens were prepared and tested. The test matrix is shown in Table 1 (Column 1-3).

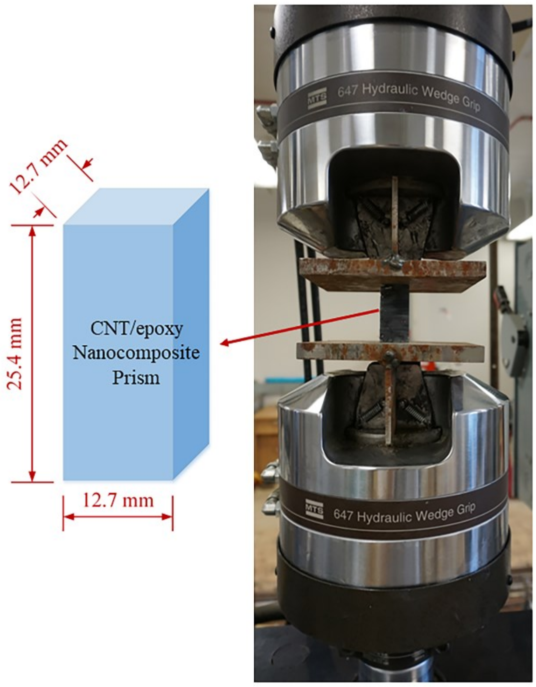

Fig. 2 Experimental configuration.

In order to gain an insight on the corrosion properties of CNT/epoxy nanocomposites, electrochemical tests were

Table 1 Compressive test results

Testing condition	Dispersion approach	CNT concentration	Compressive strength (MPa)	Modulus of elasticity (GPa)
E	\	\	41.00 ± 5.36	0.96 ± 0.04
M1	Mechanical Mixing	0.1	49.76 ± 3.54	1.09 ± 0.06
M3	Mechanical Mixing	0.3	59.71 ± 6.61	1.43 ± 0.05
M5	Mechanical Mixing	0.5	73.55 ± 8.87	1.81 ± 0.02
N1	NaDDBS functionalization	0.1	86.74 ± 8.78	2.35 ± 0.07
N3	NaDDBS functionalization	0.3	101.91 ± 17.8	2.52 ± 0.02
N5	NaDDBS functionalization	0.5	118.33 ± 7.28	2.97 ± 0.05
C1	CMC functionalization	0.1	144.05 ± 10.95	3.53 ± 0.03
C3	CMC functionalization	0.3	163.50 ± 9.13	4.13 ± 0.07
C5	CMC functionalization	0.5	186.81 ± 18.66	4.9 ± 0.09

conducted using EIS Box 300 from Gamry Instruments Inc. The specimen in electrochemical tests was a square steel sheets coated by a thin layer of CNT/epoxy nanocomposites with different dispersion approaches. The steel sheets had a dimension of 25.4 mm × 25.4 mm × 3.2 mm, and the coating thickness of all the specimens were strictly controlled at 0.5 mm. Before applying coatings, all the steel sheets were grit blasted, following cleaned by compressed air and acetone bath to create contaminate-free surfaces and strengthen the adhesion between coatings and substrates.

The corrosion inhibitive performances of CNT/epoxy nanocomposite coatings on steel substrates were analysed by Tafel polarization, which is a popular technique to estimate the corrosion rate of any anti-corrosive coatings. The Tafel polarization system was assembled with three electrode cells including the coated specimens in 3.5% NaCl solution as working electrode, stainless steel wire mesh as counter electrode, and a saturated calomel reference electrode. The voltage scanned was between ±300 mV at a scan rate of 1 mV/s with the open circuit potential after 1 hour of interruption and stabilization. The Tafel polarization curves covering slope of anodic (βa) and cathodic (βc) proportions were recorded, and three fundamental electrochemical parameters including corrosion current density (icorr), corrosion potential (Ecorr) and corrosion rate (CR) of the specimens were obtained using Gamry Instruments Framework software. In addition, two other crucial parameters, corrosion resistance (Rp) and porosity density (P.D.) of CNT/epoxy nanocomposite coatings were also calculated or estimated using the equations below to further reveal the reinforcing mechanisms of CNT addition and dispersion approaches.[48–50]

$$R_p = \frac{\beta}{i_{corr}} \tag{1}$$

$$\beta = \frac{\beta_a \times \beta_c}{2.3 \times (\beta_a + \beta_c)} \tag{2}$$

$$P.D. = \frac{R_{ps}}{R_p} \times 10^{-\left(\frac{\Delta E}{\beta_a}\right)} \tag{3}$$

Where R_{ps} is the corrosion resistance of the steel substrate without any coatings, and ΔE is potential difference between coatings and substrates.

RESULTS AND DISCUSSION

CNT Functionalization

Raman spectroscopy was carried out to quantitively differentiate the CNT functionalization effectiveness among CNTs with different dispersion approaches. Fig. 3 (a-c) show the normalized Raman spectra of ultrasonically dispersion CNTs, NaDDBS functionalized CNTs, and CMC functionalized CNTs with different CNT concentrations. As clearly seen in the figures, for each spectrum, there are two main characteristic peaks around 1348 cm^{-1} and 1585 cm^{-1} referring to D-band and G-band, respectively, which shared typical peak locations as similar previous findings.[51,52] According to literature, G-band represents inplane vibration of C-C bond in the *sp*^{2} carbon-based materials, while D-band is an indication of defective carbons in CNT structures, and it is well established that the intensity ratio between G-band and disordered induced D-band, I_D/I_G, is related to the number of localized defects or defect density in the carbon network due to structural defects or functionalization on the outer wall of CNTs.[53,54] The higher intensity ratio indicated that the physical or chemical structure of CNTs had been changed by ultrasonication or functionalization which created more defects and weakened the interactions among CNTs for a better CNT dispersion.

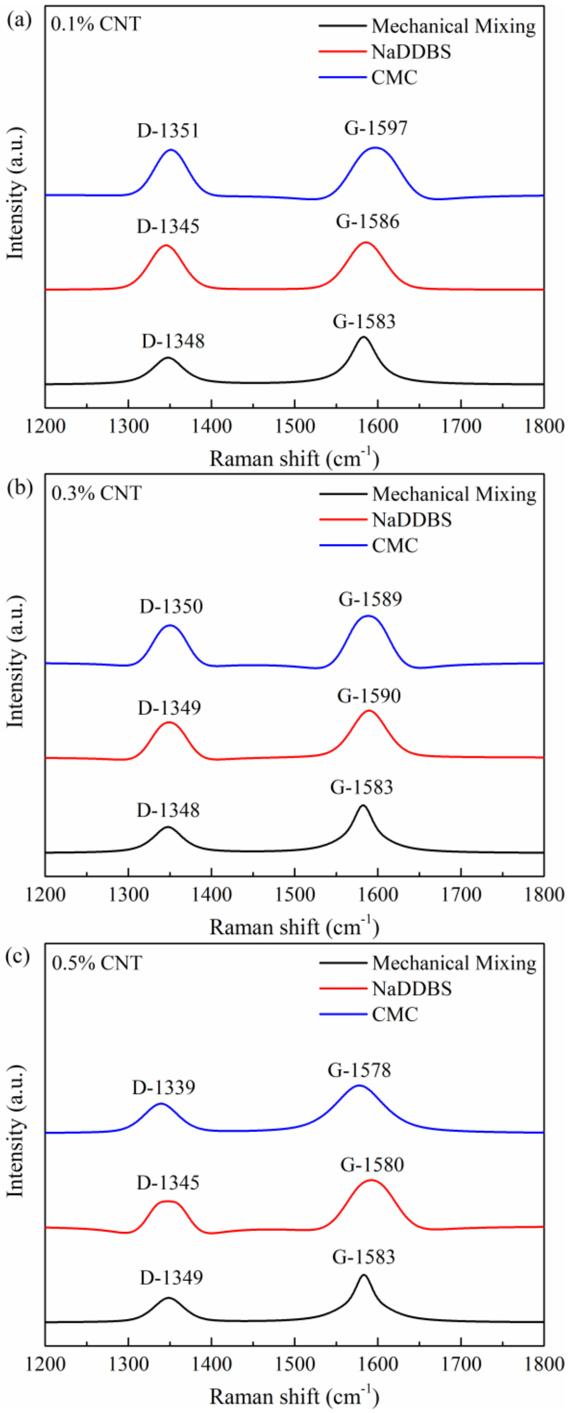

Fig. 3 Raman spectra of ultrasonically dispersion CNTs, NaDDBS functionalized CNTs, and CMC functionalized CNTs with different CNT concentrations: (a) 0.1%; (b) 0.3%; (c) 0.5%.

The change of I_D/I_G with respect to CNT concentrations is illustrated in Fig. 4. No surprisingly, the ratio kept decreasing as the addition of CNTs since CNTs were less likely to be treated by any of the dispersion approaches with higher CNT concentrations. On the other hand, by comparisons with same CNT concentration but different dispersion approaches, the intensity ratios of NaDDBS and CMC functionalization were far higher than those of mechanical mixing when the CNT concentration was 0.1% and 0.3%. Although the discrepancies among those three dispersion approaches became less significant as CNT got severely agglomerated with 0.5% concentration, CMC functionalization still acquired the highest value which was moderately higher than that of NaDDBS functionalization, and then mechanical mixing. Thus, CMC functionalization was expected to achieve the most uniform dispersion among those three dispersion approaches. The functionalization mechanism of CMCs is to reduce the Van der Waals interaction of CNTs by attaching CMCs on the external walls of CNTs. The detailed discussions and illustrations can be found in the previous work by the authors.[46]

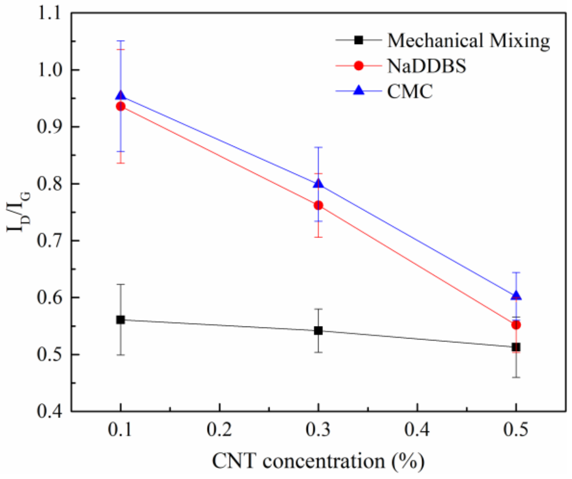

Fig. 4 The change of intensity ratio, I_D/I_G with respect to CNT concentrations.

CNT Dispersion State

The CNT dispersion states among different dispersion approaches were directly revealed by particle size analysis. Fig. 5(a-c) illustrate the particle size distributions of ultrasonically dispersion CNTs, NaDDBS functionalized CNTs, and CMC functionalized CNTs with different CNT concentrations. From the figures, irrespective of dispersion approaches, it is apparent that all the CNTs approximately ended up with a gaussian distribution with a single peak. Although some of the particle size distributions were a little skewed and not strictly symmetric, the average or mean particle size could be roughly estimated by the peak particle size with the highest volume frequency.

Fig. 6 presents the peak particle size as a function of CNT concentration. As expected, the increase of CNT concentration led to larger particle size as an indication of more serious CNT agglomeration. This tendency was valid even for functionalized CNTs because the amounts of dispersion agents were not sufficient to entirely functionalize all the entangled CNTs with relatively high CNT concentrations. However, it has been reported that simply raising the surfactant addition did improve the CNT dispersion, but too many surfactants might have a detrimental impact on the mechanical and electrical properties of the CNT reinforced polymers, which was against the purpose of surfactant usage and dispersion improvement.[47]

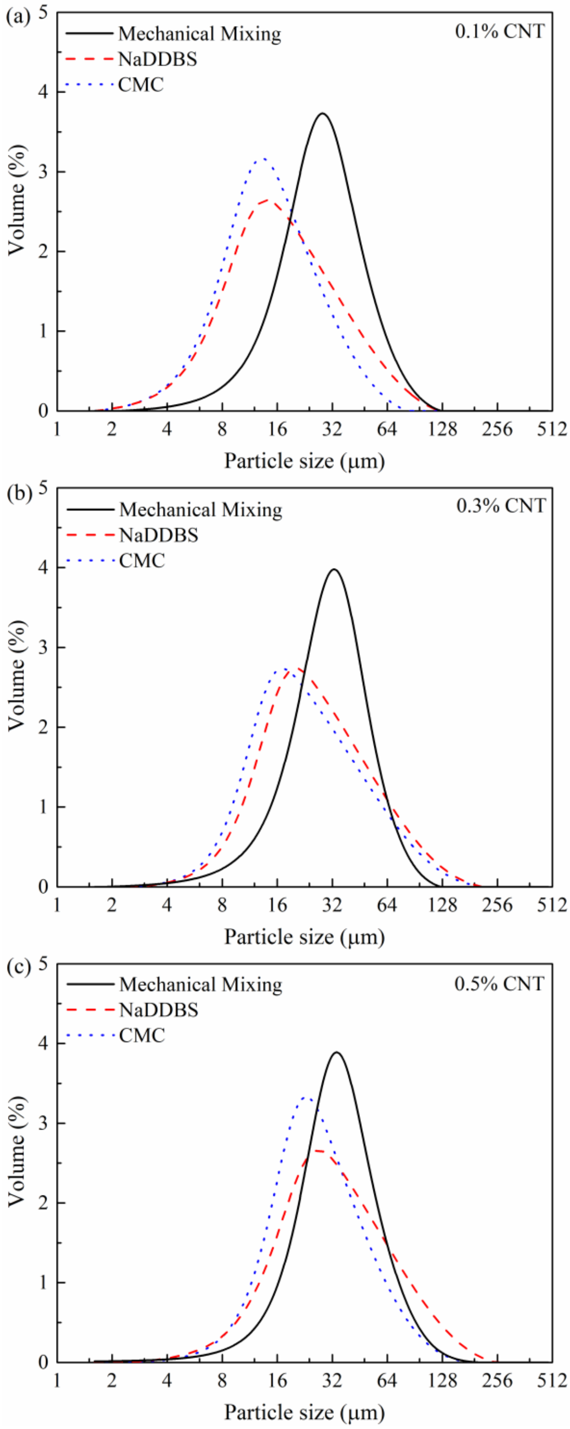

Fig. 5 Particle size distributions of ultrasonically dispersion CNTs, NaDDBS functionalized CNTs, and CMC functionalized CNTs with different CNT concentrations: (a) 0.1%; (b) 0.3%; (c) 0.5%.

By comparing the particle size distributions with the same CNT concentration but different dispersion approaches, in accordance with results from Raman spectroscopy, the peak particle sizes of CNTs with mechanical mixing were 28.38 μm, 32.88 μm, and 33.83 μm which were much larger than corresponding particle sizes of functionalized CNTs, even though the ultrasonic parameters were optimized referring to the literature.[28,29] For example, regarding 0.1 CNT addition, the peak particle sizes reduced 51% and 54% for NaDDBS and CMC functionalization respectively. The pronounced better dispersion of functionalized CNTs indicated that CNT functionalization using dispersion agents was a preferred dispersion approach compared to mechanical mixing. With respect to the two dispersion agents, CMC possessed 5%, 16%, and 14% smaller peak particle sizes for different CNT additions respectively, implying modest better dispersion states than NaDDBS correspondingly. Given that weight percentages of the two dispersion agents were the same, it was reasonable to conclude that CMC provided higher efficiency in improving CNT dispersion than NaDDBS.

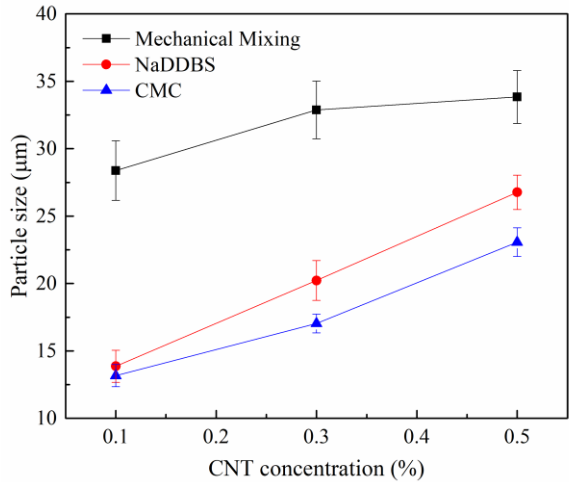

Fig. 6 The peak particle size as a function of CNT concentration.

The dispersion states of CNTs with different dispersion approaches were further verified by TEM images. Fig. 7(a-c) display the typical TEM images of 0.3% CNT with three dispersion approaches to clearly distinguish the dispersion differences. Regarding the mechanically mixed CNTs, all the CNTs were agglomerated into a huge CNT cluster and no CNT was detected outside the cluster area. As for NaDDBS functionalized CNTs, the CNT cluster size was remarkably reduced, resulting in only one medium size and one small size clusters. It is also noteworthy that some individual CNTs were observed surrounding the two CNT clusters, and those individual CNTs were believed to be sufficiently functionalized by NaDDBS as they were separated from the clusters. In the TEM images of CMC functionalized CNTs as shown in Fig. 7(c), nearly all the CNTs were dispersed homogenously and free of any CNT clusters except a small size cluster on the top edge of the image. Although CMC functionalization was not able to completely eliminate all the CNT clusters, the CNT dispersion state of CMC functionalized CNTs was largely improved. Thus, it is strongly confirmed that CMC functionalized CNTs exhibited the best dispersion state among the three dispersion approaches, although the dispersion modifying mechanism of almost all the physical functionalizing agents are the same. Those agents could attach on the outer wall of CNTs forming an amorphous layer which is able to modify CNT dispersion by weakening the surface interaction among CNTs.[27,55]

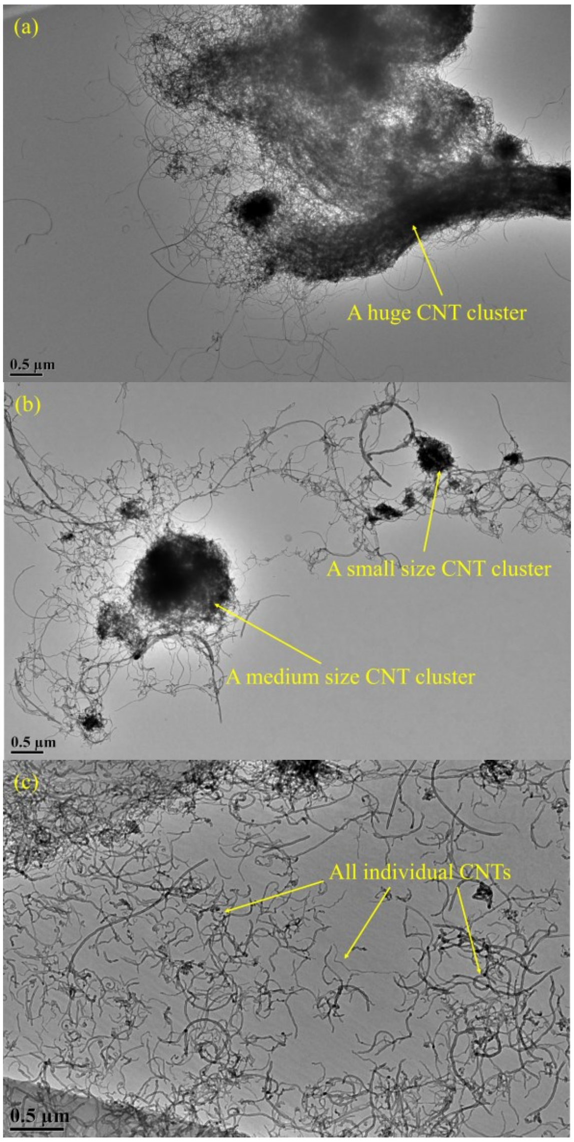

Fig. 7 TEM images of 0.3% CNT with three dispersion approaches: (a) mechanical mixing; (b) NaDDBS functionalization; (c) CMC functionalization.

Mechanical Properties of CNT/Epoxy Nanocomposites

Fig. 8(a-c) show the typical stress-strain curves of CNT/epoxy nanocomposites with mechanical mixing, NaDDBS and CMC functionalization among different CNT concentrations under compressive tests. As shown in the figures, excluding neat epoxy with a distinctive linear stress-strain relationship, all the other curves shared a similar changing trace containing an approximate linear stage followed by a non-linear stage before failure. The two-stage changing traces with CNT additions could be elucidated by CNT pull-out which is broadly regarded as one important reinforcing mechanism of CNTs.[56,57] At the beginning, CNTs and surrounding polymer matrix are well bonded as an integrity displaying as the linear stage of the stress-strain curve. As the increase of external loading, the polymer fractures after reaching the threshold of its ultimate strain. At that time, the polymer no longer deforms any more while CNTs keeps deforming, leading to the start of debonding between CNTs and the polymer. As CNTs are continually pulled out from the polymer matrix, the non-linear stage materializes with ever decreasing modulus. In the end, when debonding distance extends to the entire length of CNTs, CNTs are entirely pulled out losing its loading capacity.[58]

To further analyse the mechanical properties of CNT/epoxy nanocomposites, the stress-strain curves in the linear stage were used to calculate the modulus of elasticity, while the compressive strength was defined as the maximum stress after reaching the non-linear stage. Table 1 (Column 4-5) presents the compressive strength as well as the modulus of elasticity in all the testing conditions. Regardless of which dispersion approaches or CNT concentrations, the compressive strength of CNT/epoxy nanocomposites was significantly higher than that of neat epoxy resin. For CNT/epoxy nanocomposites with the same dispersion approaches but different CNT concentrations, higher CNT concentrations always led to higher compressive strengths, even though the dispersion state showing the opposite trend. Some previous studies indicated that the mechanical properties of CNT/epoxy nanocomposites got improved as the CNT concentration goes up to 0.75%, and then dropped beyond 1%.[11,12] In this study, the maximum CNT concentration was 0.5%. Consequently, below the specific limit, the advantage of CNT addition overwhelmed the downside of CNT dispersion implying the better compressive strength with higher CNT concentrations.

On the other hand, when comparing compressive strength of CNT/epoxy nanocomposites with the same CNT concentrations but different dispersion approaches, CMC functionalization consistently held the highest values, following by NaDDBS functionalization, while mechanical mixing remained the last. Compared to mechanical mixing and NaDDBS functionalization, the most significant improvements by CMC functionalization happened with 0.1 CNT concentration, with the increments being 189% and 66% respectively. The variations in compressive strength could be interpreted by the variations in CNT dispersion. Since premature failure always occurs at the weakness spot (initial cracks or flaws) inducing stress concentration, homogenously distributed CNTs reinforce the epoxy evenly without any noticeable weakness. Moreover, as an indication of non-uniform CNT dispersion, CNT clusters have the similar detrimental effects as imperfections in the nanocomposites. Concerning modulus of elasticity, it shared the same variations as compressive strength. Take 0.1 CNT concentration as an example, compared to mechanical mixing and NaDDBS functionalization, CNT/epoxy nanocomposites with CMC functionalization achieved 224% and 50% higher modulus respectively. Therefore, CNT/epoxy nanocomposites with CMC functionalization achieved the best mechanical properties among the three dispersion approaches, while mechanical mixing showed less reinforcing efficiency compared to CNT functionalization.

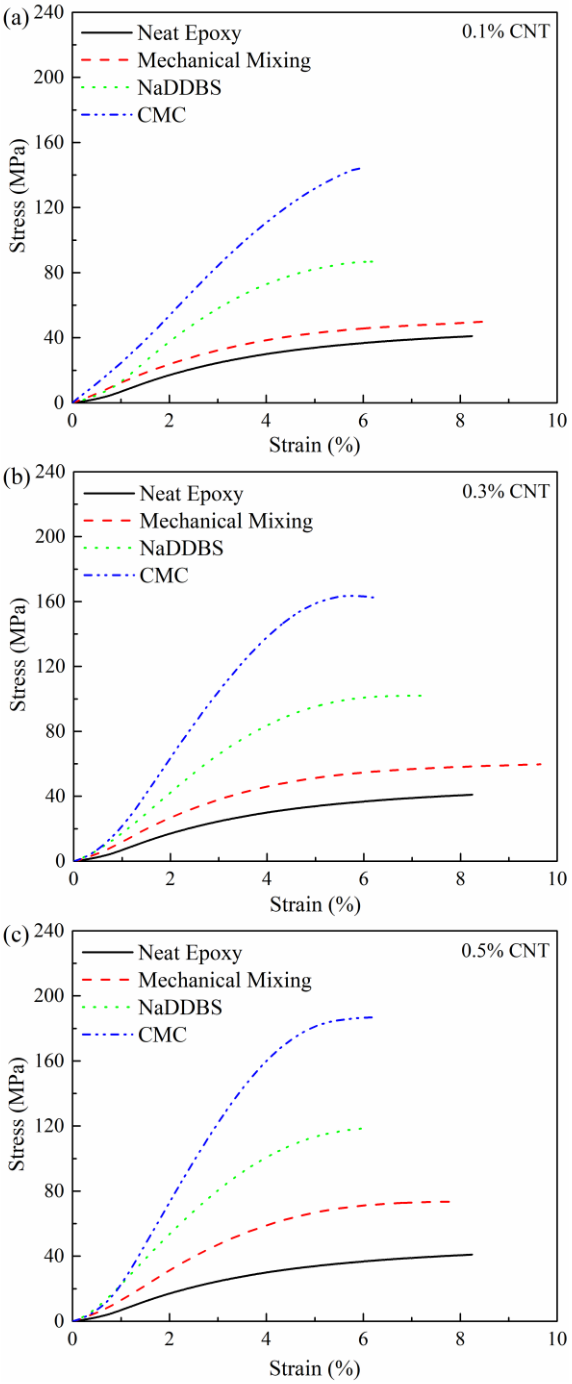

Fig. 8 Typical stress-strain curves of CNT/epoxy nanocomposites with mechanical mixing, NaDDBS and CMC functionalization among different CNT concentrations: (a) 0.1%; (b) 0.3%; (c)

0.5%.

Corrosion Properties of CNT/Epoxy Nanocomposites

Fig. 9 displays Tafel polarization curves of CNT/epoxy nanocomposites with 0.5% CNT concentration among different dispersion approaches from electrochemical corrosion tests. The corresponding electrochemical parameters are listed in Table 2. Neat epoxy coatings were also exanimated as the control group. As illustrated in the figure, all CNT/epoxy nanocomposite coatings had lower corrosion potential (E_{corr}), corrosion current density (i_{corr}), and corrosion rate (CR) than the coating made of neat epoxy resin reflecting lower tendency to corrode. Because neat epoxy resin may inevitably possess numerous voids and pores generated during curing process, suggesting a certain porosity. Although the defect free neat epoxy resin owns a notable anti-corrosive ability due to the superb corrosion resistance, in practice, those voids and pores in neat epoxy often provide a path for corrosive agents through the coating into the steel substrate, leading to the failure of corrosion protection.[59,60] However, as shown in Table 2 (Column 8), CNT addition significantly reduced the porosity density of CNT/epoxy nanocomposite coatings compared to the neat epoxy coating. The explanation lied in that CNTs or other nanofillers are able to fill voids and bridge cracks inside the epoxy coatings.[60,61] The effective physical barrier effect of CNT addition lessened the number of voids, blocked the path of electrolyte penetration, and eventually enhanced the corrosion properties of CNT/epoxy nanocomposite coatings.

Table 2 Tafel polarization parameters

Testing condition	β_a (V/dec)	β_c (V/dec)	E_{corr} (V vs SCE)	i_{corr} ($\mu A/cm^2$)	CR (mpy)	Rp (Ω cm^2)	P.D. (%)
E	0.0969	0.1745	0.983	10.264	9.382	2.639	0.143
M	0.3672	0.4924	0.853	3.698	3.380	24.730	0.088
N	0.6551	0.1622	0.584	0.611	0.558	92.514	0.022
C	0.24188	0.20111	0.419	0.234	0.214	201.031	0.011

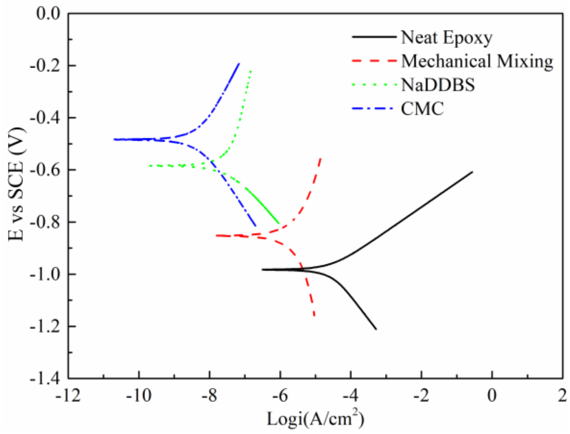

Fig. 9 Tafel polarization curves of CNT/epoxy nanocomposites with 0.5% CNT concentration among different dispersion approaches.

Regarding CNT/epoxy nanocomposite coatings among the three different dispersion approaches, it was evident that CMC functionalization gained the best corrosion performances as a result of the lowest corrosion rate (0.214 mpy) and the highest corrosion resistance (201.031 Ω cm^2). Although the corrosion performances of NaDDBS functionalization were not as good as CMC functionalization, the variations were less distinctive, given that there were considerable increments between those corrosion parameters of mechanical mixing and NaDDBS functionalization. As discussed above, CNTs could patch or fix the cracks in the nanocomposites which serves as the reinforcing mechanism for mechanical properties improvement. CNTs with better dispersion had higher possibility of covering all the imperfections leading to further porosity density reduction. It was confirmed by Table 2 (Column 8) that CMC functionalization yielded the lowest porosity density (0.011%), while mechanical mixing showed the highest among the three dispersion approaches. Therefore, CMC functionalization also had a positive effect on corrosion properties of CNT/epoxy nanocomposites due to better dispersion.

CONCLUSIONS

This paper systematically investigated the dispersion, mechanical and corrosion properties of CNT/epoxy nanocomposites with a novel CMC functionalization compared to two well-established dispersion approaches, mechanical mixing and NaDDBS functionalization, with respect to three different CNT concentrations (0.1%, 0.3%, and 0.5%).

Raman spectroscopy suggested that CMC functionalization was more effective in weakening the intense interactions among CNTs as an indication of the greater potential in modifying the CNT dispersion compared to NaDDBS functionalization and then mechanical mixing. It was observed by particle size analysis and TEM that functionalized CNTs yielded smaller cluster sizes than mechanically mixed CNTs suggesting better dispersion states, while CMC functionalization was moderately better than NaDDBS functionalization.

Mechanical tests showed that higher CNT concentrations resulted in higher compressive strength and modulus of elasticity, since the advantage of CNT addition overwhelmed the downside of CNT dispersion when CNT concentration was below 0.5%. On the other hand, when comparing different dispersion approaches, CNT/epoxy nanocomposites with CMC functionalization had better mechanical properties than the other two dispersion approaches due to more uniform dispersion, because uniformly dispersed CNTs significantly fixed cracks and flaws in the epoxy and mitigated the detrimental effect of CNT clusters.

The experimental results of electrochemical corrosion tests by Tafel polarization indicated that CNT addition tremendously reduced the porosity density and improved the corrosion properties of neat epoxy coatings. Regarding the three dispersion approaches, CNT/epoxy nanocomposites with CMC functionalization exhibited the lowest corrosion rate and highest corrosion resistance performances, while mechanical mixing showed the poorest corrosion performances as a result of the worst CNT dispersion states among the three dispersion approaches.

Overall, this paper may offer a novel CNT dispersion approach of pursuing advanced mechanical and corrosion properties of CNT/epoxy nanocomposites. In the future, large scale field applications are recommended to validate the practical potential of this technique proposed.

ACKNOWLEDGMENTS

This work was supported by the National Science Foundation under Grant No. CMMI-1750316. The findings and opinions expressed in this article are those of the authors only and do not necessarily reflect the views of the sponsors.

REFERENCES

1 Cao, D.; Malakooti, S.; Kulkarni, V.N.; Ren Y.; Lu H. Nanoindentation measurement of core–skin interphase viscoelastic properties in a sandwich glass composite. *Mech. Time-depend. Mater.* **2021**, 25, 353-363.

2 Cao, D.; Malakooti, S.; Kulkarni, V.N.; Ren Y.; Liu, Y.; Nie X.; Qian, D.; Griffith, D.T.; Lu H. The effect of resin uptake on the flexural properties of compression molded sandwich composites. *Wind Energy* **2021**, 25, 71-93.

3 Wang, X.; Xu, T.; Andrade, M.J.; Rampalli, I.; Cao, D.; Haque, M.; Roy, S.; Baughman, R.H.; Lu, H. The infterfacial shear strength of carbon nanotube sheet modified carbon fiber composites. *Chall. Mech. Time-depend. Mater.* **2021**, 2, 25-32.

4 Adams, R.D.; Peppiatt, N. A. Stress analysis of adhesive-bonded lap joints. *J. Strain Anal. Eng. Des.* **1974**, 9, 185–196.

5 Zhang, D.; Huang, Y. Influence of surface roughness and bondline thickness on the bonding performance of epoxy adhesive joints on mild steel substrates. *Prog. Org. Coatings* **2021**, 153, 106135.

6 Fu, Y.X.; He, Z.X.; Mo, D.C.; Lu, S.S. Thermal conductivity enhancement with different fillers for epoxy resin adhesives. *Appl. Therm. Eng.* **2014**, 66, 493–498.

7 Gu, H.; Ma, C.; Gu, J.; Guo, J.; Yan, X.; Huang, J.; Zhang, Q.; Guo, Z. An overview of multifunctional epoxy nanocomposites. *J. Mater. Chem. C.* **2016**, 4, 5890–5906..

8 Dong, M.; Zhang, H.; Tzounis, L.; Santagiuliana, G.; Bilotti, E.; Papageorgiou, D.G. Multifunctional epoxy nanocomposites reinforced by two-dimensional materials: A review. *Carbon N. Y.* **2021**, 185, 57–81..

9 Kumar, S.K.; Castro, M.; Saiter, A.; Delbreilh, L.; Feller, J.F.; Thomas, S.; Grohens, Y. Development of poly(isobutylene-co-isoprene)/reduced graphene oxide nanocomposites for barrier, dielectric and sensingapplications. *Mater. Lett.* **2013**, 96, 109–112.

10 Nigam, V.; Setua, D.K.; Mathur, G.N. Failure Analysis of Rubber Toughened Epoxy Resin. *J. Appl. Polym. Sci.* **2002**, 87, 861-868.

11 Sydlik, S.A.; Lee, J.H.; Walish, J.J.; Thomas, E.L.; Swager, T.M. Epoxy functionalized multi-walled carbon nanotubes for improved adhesives. *Carbon N. Y.* **2013**, 59,109–120.

12 Wang, Z.Y.; Sun, X.; Wang, Y.; Liu, J.D.; Zhang, C.; Zhao, Z.B.; Du, X.Y. Fabrication of high-performance thermally conductive and electrically insulating polymer composites with siloxane/multi-walled carbon nanotube core-shell hybrids at low filler content. *Polymer* **2022**, 262, 125430.

13 Zhang, D.; Huang, Y. The bonding performances of carbon nanotube (CNT)-reinforced epoxy adhesively bonded joints on steel substrates. *Prog. Org. Coatings* **2021**, 159, 106407.

14 Singh, N.P.; Gupta, V.K.; Singh, A.P. Graphene and carbon nanotube reinforced epoxy nanocomposites: A review. *Polymer* **2019**, 180, 121724.

15 Iijima, S. Helical Microtubules of Graphitic Carbon. *Nature* **1991**, 354, 56-58.

16 Kil, T.; Jin, D.W.; Yang, B.; Lee, H.K. A comprehensive micromechanical and experimental study of the electrical conductivity of polymeric composites incorporating carbon nanotube and carbon fiber. *Compos. Struct.* **2021**, 268, 114002.

17 Guo, Y.K.; Li, H.; Zhao, P.X.; Wang, X.F.; Astruc, D.; Shuai, M. Thermo-reversible MWCNTs/epoxy polymer for use in self-healing and recyclable epoxy adhesive. *Chinese J. Polym. Sci.* **2017**, *35*, 728–738.

18 Zhang, D.; Huang, Y.; Chia, L. Effects of carbon nanotube (CNT) geometries on the dispersion characterizations and adhesion properties of CNT reinforced epoxy composites. *Compos. Struct.* **2022**, 296, 115942.

19 Parveen, S.; Rana, S.; Fangueiro, R. A review on nanomaterial dispersion, microstructure, and mechanical properties of carbon nanotube and nanofiber reinforced cementitious composites. *J. Nanomater.* **2013**, 2013, 710175.

20 Thess, A.; Lee, R.; Nikolaev, P.; Dai, H.; Petit, P.; Robert, J. Crystalline ropes of metallic carbon nanotubes. *Science* **1996**, 273, 483-487.

21 Gao, E.; Lu, W.; Xu, Z. Strength loss of carbon nanotube fibers explained in a three-level hierarchical model. *Carbon N. Y.* **2018**, 138,134–142.

22 Zhang, D.; Huang, Y.; Wang, Y. Bonding performances of epoxy coatings reinforced by carbon nanotubes (CNTs) on mild steel substrate with different surface roughness. *Compos. Part A Appl. Sci. Manuf.* **2021**, 147, 106479.

23 Ma, P.C.; Siddiqui, N.A.; Marom, G.; Kim, J.K. Dispersion and functionalization of carbon nanotubes for polymer-based nanocomposites: A review. *Compos. Part A Appl. Sci. Manuf.* **2010**, 41, 1345–1367.

24 Yu, Z.; Di, H.; Ma, Y.; Lv, L.; Pan, Y.; Zhang, C.; He, Y. Fabrication of graphene oxide-alumina hybrids to reinforce the anti-corrosion performance of composite epoxy coatings. *Appl. Surf. Sci.* **2015**, 351, 986–996.

25 Rennhofer, H.; Zanghellini, B. Dispersion state and damage of carbon nanotubes and carbon nanofibers by ultrasonic dispersion: A review. *Nanomaterials* **2021**, 11, 1469.

26 Andrews, R.; Jacques, D.; Minot, M.; Rantell, T. Fabrication of Carbon Multiwall Nanotube/Polymer Composites by Shear Mixing. *Macromol. Mater. Eng.* **2002**, 287, 395-403.

27 Yang, H.; Yang, Y.; Liu, Y.; He, D.; Bai, J. Multi-scale study of CNT and CNT-COOH reinforced epoxy composites: dispersion state, interfacial interaction vs mechanical properties. *Compos. Interfaces.* **2021**, 28, 381–393.

28 Korayem, A.H.; Barati, M.R.; Chen, S.J.; Simon, G.P.; Zhao, X.L.; Duan, W.H. Optimizing the degree of carbon nanotube dispersion in a solvent for producing reinforced epoxy matrices. *Powder Technol.* **2015**, 284, 541–550..

29 Dassios, K.G.; Alafogianni, P.; Antiohos, S.K.; Leptokaridis, C.; Barkoula, N.M.; Matikas, T.E. Optimization of sonication parameters for homogeneous surfactant assisted dispersion of multiwalled carbon nanotubes in aqueous solutions. *J. Phys. Chem. C.* **2015**, 119, 7506–7516.

30 Jia, X.L.; Zhang, Q.; Huang, J.Q.; Zheng, C.; Qian, W.Z.; Wei, F. The direct dispersion of granular agglomerated carbon nanotubes in bismaleimide by high pressure homogenization for the production of strong composites. *Powder Technol.* **2012**, 217, 477–481.

31 Shokrieh, M.M.; Rafiee, R. Investigation of nanotube length effect on the reinforcement efficiency in carbon nanotube based composites. *Compos. Struct.* **2010**, 92, 2415–2420.

32 Haque, A.; Ramasetty, A. Theoretical study of stress transfer in carbon nanotube reinforced polymer matrix composites. *Compos. Struct*. **2005**, 71, 68–77.

33 Park, K.C.; Hayashi, T.; Tomiyasu, H.; Endo, M.; Dresselhaus, M.S. Progressive and invasive functionalization of carbon nanotube sidewalls by diluted nitric acid under supercritical conditions. *J. Mater. Chem.* **2005**, 15, 407–411.

34 Gabriel, G.; Sauthier, G.; Fraxedas, J.; Moreno-Mañas, M.; Martínez, M.T.; Miravitlles, C.; Casabó, J. Preparation and characterisation of single-walled carbon nanotubes functionalised with amines. *Carbon N. Y.* **2006**, 44, 1891–1897.

35 Ma, P.C.; Kim, J.K.; Tang, B.Z. Functionalization of carbon nanotubes using a silane coupling agent. *Carbon N. Y.* **2006**, 44, 3232–3238.

36 Han, B.; Yu, X. Effect of surfactants on pressure-sensitivity of CNT filled cement mortar composites. *Front. Mater.* **2014**, 1.

37 Carilli, C.L.; Lewis, G.F.; Djorgovski, S.G.; Mahabal, A.; Cox, P.; Bertoldi, F.; Omont, A. A molecular Einstein ring: Imaging a starburst disk surrounding a quasi-stellar object. *Science* **2003**, 300, 773–775.

38 Imtiaz, S.; Siddiq, M.; Kausar, A.; Muntha, S.T..; Ambreen, J.; Bibi, I. A review featuring fabrication, properties and applications of carbon nanotubes (CNTs) reinforced polymer and epoxy nanocomposites. *Chinese J. Polym. Sci.* **2018**, 36, 445–461.

39 Chen, Y.; Wei, W.; Zhu, Y.; Luo, J.; Liu, X. Noncovalent functionalization of carbon nanotubes via co-deposition of tannic acid and polyethyleneimine for reinforcement and conductivity improvement in epoxy composite. *Compos. Sci. Technol.* **2019**, 170, 25–33.

40 Qi, Z.; Tan, Y.; Wang, H.; Xu, T.; Wang, L.; Xiao, C. Effects of noncovalently functionalized multiwalled carbon nanotube with hyperbranched polyesters on mechanical properties of epoxy composites. *Polym. Test.* **2017**, 64, 38–47.

41 Monthioux, M.; Smith, B.W.; Burteaux, B.; Claye, A.; Fischer, J.E.; Luzzi, D.E. Sensitivity of single-wall carbon nanotubes to chemical processing: an electron microscopy investigation. *Carbon N. Y.* **2001**, 39, 1251-1272.

42 Cha, J.; Jin, S.; Shim, J.H.; Park, C.S.; Ryu, H.J.; Hong, S.H. Functionalization of carbon nanotubes for fabrication of CNT/epoxy nanocomposites. *Mater. Des*. **2016**, 95, 1–8.

43 Chen, B.; Chen, J.; Li, J.Y.; Tong, X.; Zhao, H.C.; Wang, L.P. Oligoaniline assisted dispersion of carbon nanotubes in epoxy matrix for achieving the nanocomposites with enhanced mechanical, thermal and tribological properties. *Chinese J. Polym. Sci.* **2017**, 35, 446-454.

44 Rahman, M.S.; Hasan, M.S.; Nitai, A.S.; Nam, S.; Karmakar, A.K.; Ahsan, M.S.; Shiddiky, M.J.A.; Ahmed, M.B.; Recent Developments of Carboxymethyl Cellulose. *Polymers* **2021**, 13, 1345.

45 Minami, N.; Kim, Y.; Miyashita, K.; Kazaoui, S. Nalini, B. Cellulose derivatives as excellent dispersants for single-wall carbon nanotubes as demonstrated by absorption and photoluminescence spectroscopy. *Appl. Phys. Lett.* **2006**, 88, 093123.

46 Zhang, D.; Huang, Y. Dispersion characterizations and adhesion properties of epoxy composites reinforced by carboxymethyl cellulose surface treated carbon nanotubes. *Powder Technol*. **2022**, 404, 117505.

47 Chia, L.; Huang, Y.; Lu, P.; Bezbaruah, A.N. Surface Modification of Carbon Nanotubes Using Carboxymethyl Cellulose for Enhanced Stress Sensing in Smart Cementitious Composites. *IEEE Sens. J.* **2021**, 21, 15218–15229.

48 Creus U, J.; Mazille, H.; Idrissi, H. Porosity evaluation of protective coatings onto steel, through electrochemical techniques. *Surf. Coat. Technol.* **2000**, 130, 224-232.

49 Ranganatha, S.; Venkatesha, T. V.; Vathsala, K. Development of electroless Ni-Zn-P/nano-TiO 2 composite coatings and their properties. *Appl. Surf. Sci.* **2010**, 256, 7377–7383.

50 Mazaheri, H.; Allahkaram, S.R. Deposition, characterization and electrochemical evaluation of Ni-P-nano diamond composite coatings. *Appl. Surf. Sci*. **2012**, 258, 4574–4580.

51 Pizzutto, C.E.; Suave, J.; Bertholdi, J.; Pezzin, S.H.; Coelho, L.A.F.; Amico, S.C. Study of epoxy/CNT nanocomposites prepared via dispersion in the hardener. *Mater. Res.* **2011**, 14, 256–263.

52 Jojibabu, P.; Zhang, Y.X.; Rider, A.N.; Wang, J.; Gangadhara Prusty, B. Synergetic effects of carbon nanotubes and triblock copolymer on the lap shear strength of epoxy adhesive joints. *Compos. Part B Eng*. **2019**, 178, 107457.

53 Bourchak, M.; Juhany, K.A.; Salah, N.; Ajaj, R.; Algarni,A.; Scarpa, F. Determining the tensile properties and dispersion characterization of CNTs in epoxy using Tem and Raman spectroscopy. *Mech. Compos. Mater.* **2020**, 56, 215–226

54 Jorio, A.; Saito, R. Raman spectroscopy for carbon nanotube applications. *J. Appl. Phys.* **2021**, 129, 021102.

55 Mallakpour, S.; Soltanian, S. Surface functionalization of carbon nanotubes: Fabrication and applications. *RSC Adv.* **2016**, 6, 109916–109935.

56 Cha, J.; Jun, G.H.; Park, J.K.; Kim, J.C.; Ryu, H.J.; Hong, S.H. Improvement of modulus, strength and fracture toughness of CNT/Epoxy nanocomposites through the functionalization of carbon nanotubes. *Compos. Part B Eng.* **2017**, 129, 169–179.

57 Shokrian, M.D.; Shelesh-Nezhad, K.; Najjar, R. Effect of CNT dispersion methods on the strength and fracture mechanism of interface in epoxy adhesive/Al joints. *J. Adhes. Sci. Technol.* **2019**, 33, 1394–1409.

58 Chen, X.; Beyerlein, I.J.; Brinson, L.C. Curved-fiber pull-out model for nanocomposites. Part 1: Bonded stage formulation, *Mech. Mater.* **2009**, 41, 279–292.

59 Ramezanzadeh, B.; Bahlakeh, G.; Ramezanzadeh, M. Polyaniline-cerium oxide (PAni-CeO2) coated graphene oxide for enhancement of epoxy coating corrosion protection performance on mild steel. *Corros. Sci.* **2018**, 137, 111–126.

60 Jeon, H.R.; Park, J.H.; Shon, M.Y. Corrosion protection by epoxy coating containing multi-walled carbon nanotubes. *J.*

Ind. Eng. Chem. **2013**, 19, 849–853.

61 Moradi, M.H.; Aliofkhazraei, M.; Toorani, M.; Golgoon, A.; Rouhaghdam, A.S. SiAlON–epoxy nanocomposite coatings: Corrosion and wear behavior. *J. Appl. Polym. Sci.* **2016**, 133, 43855.

Graphical Abstract Use Only

Effect of carboxymethyl cellulose (CMC) functionalization on dispersion, mechanical, and corrosion properties of CNT/epoxy nanocomposites

Dawei Zhang[a], Leonard Chia[a], and Ying Huang[a*]